



Internal stress induced in the process of boron coating

H. Kemi, C. Sasaki, M. Kitamura, N. Satomi¹, Y. Ueda^{*}, M. Nishikawa

Graduate School of Engineering, Osaka University, 2-1 Yamada-Oka, Suita, Osaka 565-0871, Japan

Abstract

Internal stresses induced in boron films formed by vacuum deposition were studied to find the generation mechanism of compressive stresses by an optically levered laser method. It was found that the internal stresses of boron thin films changed from tensile to compressive with increasing substrate temperatures and decreasing deposition rates. Deliberate addition of oxygen gas in an atmosphere with a pressure of 0.02 mTorr did not clearly change internal stresses, though oxygen content was increased. According to the observation by a transmission electron microscope (TEM), the film structure was in an amorphous state based on icosahedral subunits. An interatomic distance for the high deposition rate (0.5 nm/s) was slightly larger by 1.7% than that for the low deposition rate (0.06 nm/s). This result seems consistent with a film formation model based on adatom migration. © 1999 Elsevier Science B.V. All rights reserved.

Keywords: Boron coating; Internal stress

1. Introduction

It is well known that boronization of first walls is very effective to reduce oxygen contamination in tokamak [1–5] and other fusion plasma devices [6]. Plasma parameters such as energy confinement time have been improved significantly with boronization. The thickness of boron coatings for present devices is an order of 100 nm, which would be enough for pulsed operation. For future fusion reactors, however, much thicker boron coatings could be needed because of the necessity of steady state operations, even though redeposition of eroded boron and real time boronization [7] would be considered.

Thin films are generally in a state of stress, which sometimes causes adhesion failure or exfoliation. These mechanical failure would be a fatal problem for future reactors with thick boron coatings. Therefore, it is important to investigate the internal stress in boron coatings and to find the deposition conditions with good adhesion and no exfoliation. The mechanical properties

of boron coatings, however, have not sufficiently been understood.

In our previous work [8], concurrent effects of hydrogen and helium bombardment on internal stress of boron films were studied by an optically levered laser method. It was found that hydrogen ion irradiation with energies of 100–400 eV resulted in the large compressive stress due to ion peening effects [9]. On the other hand, helium ion irradiation with energies of 100–400 eV reduced the compressive stress.

These results partly account for the generation mechanism of compressive stress in boron coatings. The stresses observed in the metallic films and some semi-conducting materials (silicon and germanium) by vacuum deposition are almost always tensile [10]. So the boron seems to be an exceptional material that can be deposited in a state of compressive stresses. There still remain some problems to be solved for the induced compressive stresses and their relaxation.

In this study, the stress in the boron films formed by vacuum deposition was observed in detail to find the mechanism of stress induced under several deposition condition such as substrate temperature and deposition rate. The effect of oxygen impurity in an atmosphere on internal stresses from the viewpoint of oxygen gettering near the plasma surface was also investigated. In addition, the internal structure of boron thin films on the deposition rate is discussed.

^{*} Corresponding author. Tel.: +81 6 6879 7236; fax: +81 6 6879 7867; e-mail: yueda@ppl.eng.osaka-u.ac.jp

¹ Department of Mechanical Engineering, College of Industrial Technology, 1-27-1 Nishikoya, Amagasaki, Hyogo 661-0047, Japan.

2. Experimental methods

Stress measurements were carried out in process for boron films formation by the vacuum deposition method. Fig. 1 shows a schematic diagram of boron deposition and real-time internal stress measurements system. The boron source materials were evaporated by a conventional 270° deflection type EB gun (4 kV, 500 mA). The substrates were Mo plates with the dimensions of 9.5 × 50 × 0.4 mm. Temperature of the substrates was able to be regulated from 150°C to 900°C by a tungsten heater. Substrate temperature was carefully controlled within 3°C and its fluctuation effect on internal stress can be ignored. The stainless steel vessel was pumped down to less than 1 × 10⁻⁴ Pa by a turbo molecular pump. Film thickness was measured by a thickness monitor with a quartz crystal oscillator. In addition, the film thickness was measured afterwards in air by a surface profile meter (Veeco, Dektak3) to make a precise calibration.

The stress was measured from the change in curvature induced in the substrate by using an optically levered laser method. The light source was a He–Ne laser with a power of 0.5 mW. The laser beam was focused on the detector by the cylindrical lens with 1000 mm focal length. The resulting translation of the reflected beam was measured by a position sensitive detector (PSD, Hamamatsu S3931) with a sensitive area of 1 × 6 mm² and spatial resolution of 30 μm. The formula to calculate total stress from the curvature of substrates was shown in Ref. [11].

3. Experimental results

The results of the total stress (the integral of the stress over the thickness of the film) are plotted against

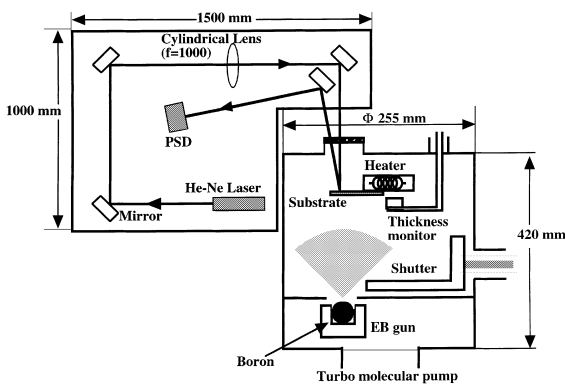


Fig. 1. Experimental setup for in-situ internal stress measurement.

film thickness for the vacuum deposition with deposition rate as a parameter in Fig. 2. The positive (negative) number of the total stress indicates that the stress is tensile (compressive). Fig. 2 shows that the stress changes from compressive to tensile, as the deposition rate is increased from 0.06 to 0.58 nm/s, the stress changes from compressive to tensile. For all deposition rate conditions, the total stress changes almost linearly with the thickness, which indicates that the stresses are uniformly induced regardless of compressive or tensile stress. It suggests that the interfacial effects, such as lattice misfits and dislocations between the film and the substrate, scarcely contribute to the stress. By taking a close look at evolution of differential coefficients of stress-thickness curves, it is found that they increase slightly with the thickness of the films. Although the reason of this change is not known, this gives only a minor effect to our results.

In general, stresses in films are strongly affected by substrate temperature. Fig. 3 shows the total stress

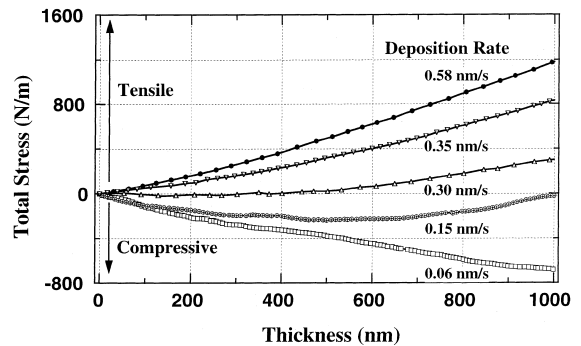


Fig. 2. Total stress as a function of boron film thickness with deposition rates as a parameter.

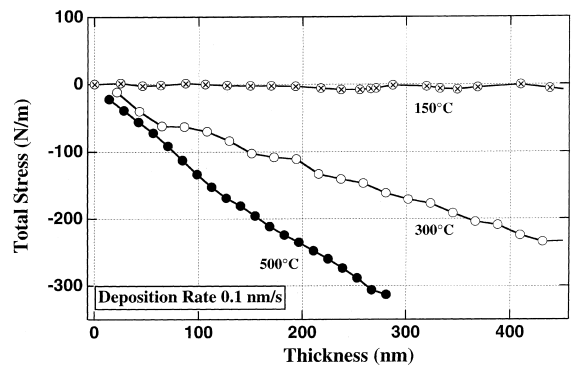


Fig. 3. Total stress as a function of boron film thickness with substrate temperatures as a parameter.

against film thickness with a substrate temperature as a parameter for the deposition rate of 0.1 nm/s. As substrate temperature increases, the total stress changes from tensile to compressive. It is noted that the higher substrate temperature did not result in the relaxation of internal stress, but resulted in higher compressive stress. These data may indicate that the compressive stress is caused by enhanced adatom mobility due to increased substrate temperature.

One of the generation mechanisms of internal stresses of thin films, especially for compressive stress, is considered due to an impurity effect [10]. It has been observed that aluminium films deposited in an atmosphere with deliberate addition of oxygen show compressive stresses. We also tried to find the effect of oxygen gas in an atmosphere during deposition. Fig. 4 shows the total stress at the thickness of 400 nm as function of deposition rate with different oxygen gas pressures and substrate temperatures. It was found that the dependence of total stress on deposition rates and substrate temperatures with 2.7×10^{-3} Pa oxygen gas were similar to those without oxygen gas (base pressure is about 10^{-4} Pa). This result suggests that the introduction of oxygen gas to the pressure of 2.7×10^{-3} Pa did not affect the internal stress of boron thin films.

Oxygen content in boron films were measured by X-ray photoelectron spectroscopy (XPS, KRATOS AXIS 165). Boron films deposited without oxygen gas did not contain observable oxygen (less than 1%), while boron films in an oxygen atmosphere contains 5–20% oxygen. The dependence of oxygen content on deposition parameters, however, did not show up clearly. From chemical shift of the observed oxygen peaks of XPS measurements, oxygen atoms could exist in boron films as molecules; oxygen was not in a covalent state with

boron. This might relate to the reason why atmospheric oxygen did not clearly affect internal stresses of boron films in our experiments.

4. Discussions

Amorphous films usually show density less than bulk material density, since their structures are rich in defects such as large micropores and open voids. Tensile stress in the amorphous films is due partly to an attractive interatomic force in these defects. Müller has recently used molecular dynamic computer simulations to explain the internal stress as a relation of the film structure [12]. He showed that with increasing substrate temperature and with decreasing deposition rate the film resulted in a transition from a porous film to a densely packed film with less microvoids. These structures can be understood in terms of adatom mobility, which depends on temperature and an atomic self-shadowing effect. From a certain temperature onward, the migration rate of adatom is large enough to surpass the rate of void incorporation during growth, resulting in denser films with higher temperature. In addition, as the deposition rate is decreased, the self-shadowing effect of adatom is less significant; densely packing films are formed.

Therefore, one of the important physical properties for clarifying the mechanism of internal stress is density of boron thin films. We tried to measure the film density from the deposited mass of boron and the thickness of films. The deposited mass was measured by the oscillating quartz resonator placed near the substrate. The thickness of the thin films were measured by a surface profile monitor. The results are shown in Fig. 5. The trend of the change of film density is not clear due to large errors even in a wide range of deposition rate, where the stresses also change significantly. The large error bars were caused by the error of the thickness measurements. Measured average density is about 2.0 ± 0.1 g/cm³, which is quite less than the reported value of bulk amorphous boron (2.35 g/cm³).

In order to analyse detailed film structure as well as boron film density, a transmission electron microscope (TEM, JEOL, JEM-2010) was employed. A diffraction image of boron thin films showed halo patterns, which indicated that our boron thin films were in an amorphous state. From this diffraction image, we calculated an effective radial distribution function (RDF) expressing the distribution of boron atoms at a radial position r from any reference boron atoms. The results are shown in Fig. 6 for the cases of a high deposition rate (0.5 nm/s (a)) and a low deposition rate (0.06 nm/s (b)) with a calculation result based on an icosahedral subunit model (B₁₂ model) [13]. The first peaks at 0.184 nm (Fig. 6(a)) and 0.181 nm (Fig. 6(b)) correspond to inter-atomic distances between the first nearest neighbours and show

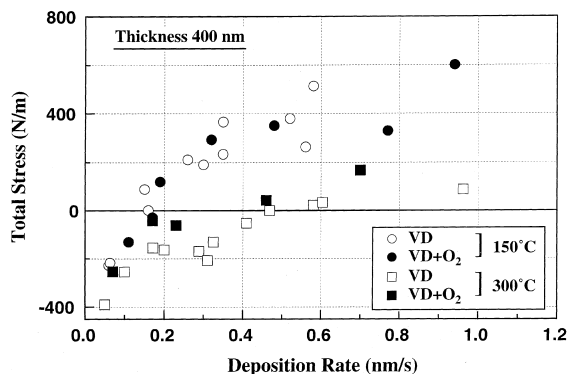


Fig. 4. Total stress at the thickness of 400 nm as a function of deposition rates. Open symbols denote the data for vacuum deposition (VD), while closed symbols denote the data for vacuum deposition with deliberate addition of oxygen gas (0.02 mTorr).

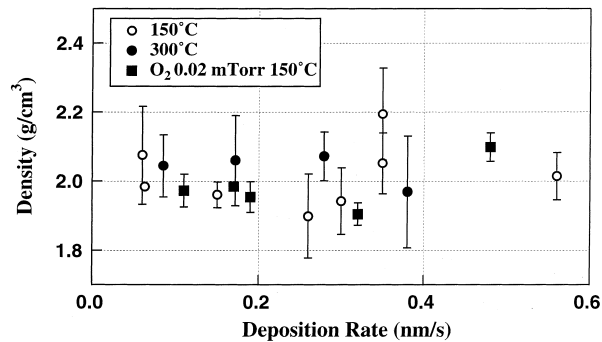


Fig. 5. Boron film density as a function of deposition rates. Error bars are mainly caused by thickness measurements of the films by a surface profile meter.

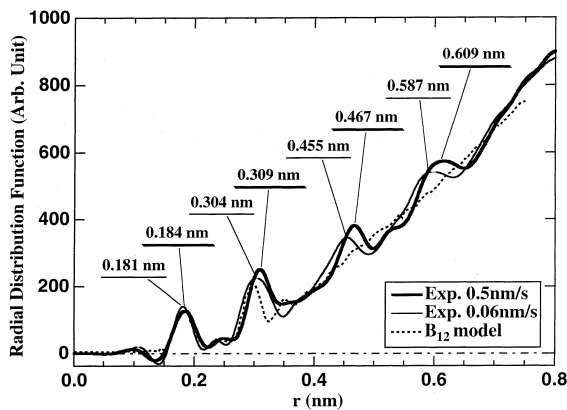


Fig. 6. Effective radial distribution function (RDF) of boron thin films measured by TEM for the deposition rate of 0.5 and 0.06 nm/s with a calculation result based on an icosahedral subunit model (B_{12} model).

a good correlation with that for the model. The second peaks at 0.309 nm (Fig. 6(a)) and 0.304 nm (Fig. 6(b)) for the second nearest neighbours are slightly longer distance than that for the model. The third and fourth peaks could describe the medium-range order in the amorphous structure.

For the analysis of an atomic structure, determination of a coordination number is important. The coordination number can be obtained by integrating RDF around each peak position, which was approximated by a Gaussian curve in our study. An estimation of the coordination numbers, however, is vulnerable to a truncation error due to finite limits of a Fourier transformation of an interference function, which results in ripples in RDF, for example, appeared around 0.10 nm (Fig. 6(a),(b)). Due to these ripples, the integration gives the smaller number than the real coordination number. These differences could be roughly less than 20%. First

coordination numbers of 4.9 (Fig. 6(a)) and 5.3 (Fig. 6(b)) were obtained from our results, while second coordination numbers were 15.0 (Fig. 6(a)) and 12.6 (Fig. 6(b)). The similarity between our RDF results and the B_{12} model could indicate the existence of the icosahedron as a subunit in amorphous boron, in which first and second coordination numbers can be considered to be 6 and 15, respectively.

Concerning inter-atomic distance deduced from RDF, the peak radius of RDF for the high deposition rate (Fig. 6(a)) is slightly larger than that for the low deposition rate (Fig. 6(b)), which is observed for all peaks. However, the difference between the high and the low deposition rate cases is only 1.7% for the first and the second peaks, corresponding to about 5% difference in volume. This small change in volume is consistent with the result of density measurements, which shows no significant change with deposition rates. In a neutron diffraction study [13], the structure of bulk amorphous boron would be based on β -rhombohedral structures with some disorder occurring in the linking between B_{12} icosahedral subunits. RDF of our TEM results shown in Fig. 6 is quite similar to that obtained by this study for all peak positions, which suggests that boron films in our experiments have basically similar amorphous structures to that of bulk boron materials with more micropores and voids because of low density. From the fact that film density only shows slight change (within 5%) with deposition rate, it could be suggested that small scale strain induced in the boron films depending on the deposition rates would relate to internal stresses. In consideration of Young's modulus of boron (less than 5×10^{11} Pa) and the internal stress of the order of 1 GPa in our experiments, minimum strain of boron giving the internal stress of 1 GPa is about 0.2%, which does not contradict with density measurements and TEM results considering ambiguity of mechanical properties of amorphous boron and experimental errors.

5. Conclusion

Main conclusions obtained by this study are as follows:

(1) Internal stresses of boron thin films formed by vacuum deposition changed from tensile to compressive with increasing substrate temperatures and decreasing deposition rates.

(2) Although atmospheric oxygen (2.7×10^{-3} Pa) increased oxygen content in boron thin films to 5–20 at%, internal stresses were not clearly changed with oxygen content.

(3) TEM observation showed boron thin films were in an amorphous state based on icosahedral subunits. An interatomic distance for the high deposition (0.5 nm/s) rate was slightly larger by 1.7% than that for the low deposition rate (0.06 nm/s), which seems consistent with the film formation model based on adatom migration.

For the boronization of first walls by physical vapour deposition process by using solid boron targets, the stress free condition is dependent on both deposition rates and temperature. It is noted that increase in temperature does not always cause relaxation of internal stresses in the temperature range from 150°C to 500°C, but simply change internal stresses from tensile to compressive.

References

- [1] M. Saidoh, N. Ogiwara, M. Shimada, T. Arai, H. Hiratsuka, et al., *Jpn. J. Appl. Phys.* 32 (1993) 3276.
- [2] H.F. Dylla, M.G. Bell, R.J. Hawryluk, K.W. Hill, S.J. Kilpartrick, et al., *J. Nucl. Mater.* 176&177 (1990) 337.
- [3] G.L. Jackson, J. Winter, K.H. Burrell, J.C. DeBoo, C.M. Greenfield, et al., *J. Nucl. Mater.* 196–198 (1992) 236.
- [4] U. Schneider, W. Poschenrieder, M. Bessenrodt-Weberpals, J. Hofmann, A. Kallenbach, et al., *J. Nucl. Mater.* 176&177 (1990) 350.
- [5] J. Winter, H.G. Esser, L. Könen, V. Philipps, H. Reimer, et al., *J. Nucl. Mater.* 162–164 (1989) 713.
- [6] N. Noda, A. Sagara, H. Yamada, Y. Kubota, N. Inoue, et al., *J. Nucl. Mater.* 220–222 (1995) 623.
- [7] A. Sagara, Y. Hasegawa, K. Tsuzuki, N. Inoue, H. Suzuki, et al., *J. Nucl. Mater.* 241–243 (1997) 972.
- [8] N. Satomi, K. Tanaka, M. Kitamura, M. Nishikawa, *J. Nucl. Mater.* 241–243 (1997) 1138.
- [9] H. Windischmann, *J. Appl. Phys.* 62 (1987) 1800.
- [10] F.M. D'heurle, J.M. Harper, *Thin Solid Films* 171 (1989) 81.
- [11] N. Satomi, S. Sato, K. Tanaka, M. Saidoh, M. Nishikawa, *J. Nucl. Mater.* 220–222 (1995) 752.
- [12] K.H. Müller, *J. Appl. Phys.* 58 (1985) 2573.
- [13] R.G. Delaplane, U. Dahlborg, W.S. Howells, T. Lundström, *J. Non-Cryst. Solids* 106 (1988) 66.